Renewable energy supply (pv) integration with building energy management: modeling and intelligent control of electrical storage

Đặng Hoàng Anh, Nguyễn Đình Quang, Đinh Văn Bình, Benoit Delinchant, Frederic Wurtz, Nguyễn Xuân Trường

▶ To cite this version:

Đặng Hoàng Anh, Nguyễn Đình Quang, Đinh Văn Bình, Benoit Delinchant, Frederic Wurtz, et al.. Renewable energy supply (pv) integration with building energy management: modeling and intelligent control of electrical storage. Vietnam Academy of Science and Technology Journal of Science and Technology, 2015, 53 (6A), pp.173- 187. hal-01410047

HAL Id: hal-01410047
https://hal.science/hal-01410047

Submitted on 6 Dec 2016

HAL is a multi-disciplinary open access archive for the deposit and dissemination of scientific research documents, whether they are published or not. The documents may come from teaching and research institutions in France or abroad, or from public or private research centers.

L'archive ouverte pluridisciplinaire **HAL**, est destinée au dépôt et à la diffusion de documents scientifiques de niveau recherche, publiés ou non, émanant des établissements d'enseignement et de recherche français ou étrangers, des laboratoires publics ou privés.

RENEWABLE ENERGY SUPPLY (PV) INTEGRATION WITH BUILDING ENERGY MANAGEMENT: MODELING AND INTELLIGENT CONTROL OF ELECTRICAL STORAGE

Đặng Hoàng Anh[1,*], Nguyễn Đình Quang [2, 3], Đinh Văn Bình[4], Benoit Delinchant[4], Frederic Wurtz[4], Nguyễn Xuân Trường[3]

[1]*Viện Công Nghệ Trường Đại học Công Nghiệp Hà Nội (HIT)*
[2]*Viện Khoa học năng lượng (IES), Viện Hàn lâm Khoa học và Côngnghệ Việt Nam (VAST)*
[3]*Đại học Khoa học và Công nghệ Hà Nội (USTH)*
[4]*Grenoble Electrical Engineering Laboratory (G2Elab)*

[*]Email: *danghoanganh@haui.edu.vn*

ABSTRACT

In building energy management, the electrical storage is important to ensure power supply continuity and reduce cost of electrical consumption. Therefore, an electrochemical battery model is highly recommended for our main objectives, which can contribute to simulate the impact of electrical storage in the building. In our framework, we have developed a complete solution for the electrical optimal management, including prediction, optimization, and real-time management of an electrical storage system with photovoltaic generation. We firstly present the models required to predict consumption patterns, production and storage. Then, under our experimental platform, we detail the predictive control algorithm, monitoring solutions and equipment control, as well as the results obtained. In near future, this research will be applied for the "Micro Smart Grid Development and Application for Building Energy Management" project (USTH, HIT, G2Elab and VAST).

Keywords: building energy management, electrical storage, renewable energy, demand response, energy autonomy.

1. INTRODUCTION

The building is a major sector in the power system and have an important role in solving problems related to the operation of power systems such as peak consumption and blackout. In addition to reducing consumption, reducing peak demand will go through the smoothing of daily consumption curves through actions of Demand Response (DR) as moving loads to times of low consumption [1] [2].

Decentralization of energy production at the user level (especially in buildings) due to the integration of renewable energy, introduces additional difficulties in managing the overall production of electric network [3]. On the other hand, it can have degrees on consumption adjustment and energy autonomy.

The smart building must be equipped with the following capabilities related to: energy storage; energy consumption and load shedding; generation [4] [5].

These capabilities will be coupled with:

- energy market , market offloading capability;
- prediction: each node must be able to anticipate the capacity of production, storage and consumption.
- real-time control : each node must be able to dynamically adjust the production capacity , storage , consumption and load shedding to respond to hazards that may be related to incidents (loss of production units, meteorology, ...)

The storage medium can be heat capacity, it is indeed possible to anticipate heating using thermal inertia [6]. The storage medium can be electrochemical batteries, and in this case, the use of existing batteries is preferred. For example, vehicle-to-grid (V2G), operates the electric vehicle batteries [7] [8].

In our framework, we have developed a complete solution for the electrical optimal management, including prediction, optimization, and real-time management of an electrical storage system with photovoltaic generation. We firstly present the models required to predict consumption patterns, production and storage. Then, under our experimental platform, we detail the predictive control algorithm, monitoring solutions and equipment control, as well as the results obtained.

2. PREDICTION MODELS

In this section, model used for electrical energy prediction are briefly presenter (photovoltaic production, load consumption, electrical price). The energy storage systems, that we want to control, which is electrochemical batteries, have been modeled more accurately in order to have access to important parameters like the state of charge (SOC) and state of health (SOH), is detailed in section III.

2.1 Photovoltaic production

The power output of the PV generator is related with solar irradiance and ambient temperature. From these forecast data and manufactures data for PV modules, we can predict this production in according to the following equation [6]:

$$P_{PV} = \eta_g N A_m G_t \qquad (1)$$

where η_g is the instantaneous PV generator efficiency. This value is represented as follows [10]:

$$\eta_g = \eta_r \eta_{pt}(1-\beta_t(T_a - T_r)) - \beta_t G_t (\frac{NOCT-20}{800})(1-\eta_r\eta_{pt})) \quad (2)$$

2.2 Load prediction

From classroom internet calendar, we can obtain the occupant plan (1 or 0 for each hour) and number of students who will be using classroom computers for the next day. By supposing an average power load consumption of each used laptop of 30W, we can predict the load consumption (3) and its profile.

$$P_{load} = 30 \times ns \tag{3}$$

2.3 Electrical price

In electrical market of developed country, the electrical price is depended on energy demand and furnished by electrical distributor (EPEX www.epexspot.com).

3. BATTERY MODEL

In simulation and application of electrical storage, the preferred electrical model of battery is electrical capacity, which is simple and describes energy balance in charging and discharging process. However, this model cannot describe accurately the functional states of the battery at each moment (state of charge, state of health) and some functional conditions (overvoltage, overcurrent) for predictive and feedback control. For example (Figure 1), in the constant voltage stage, charge current depends highly on battery property, and real charge time is much longer than estimated charge time by using an electrical capacity model. To reach these proposed goals and take into account the battery typical characteristics, a physical model is required but has to be as simple as possible.

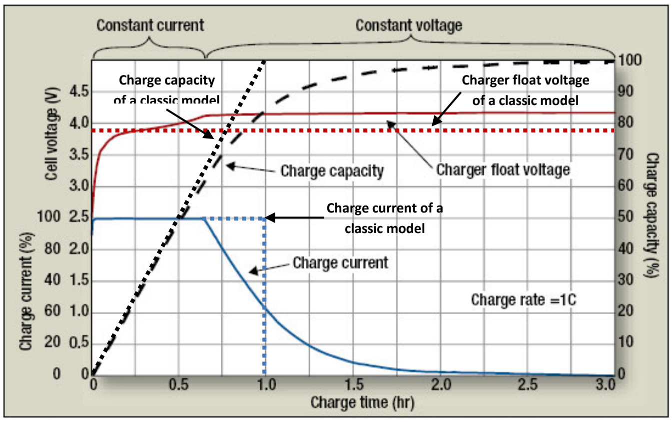

Figure 1. Charge profile of a Li-ion battery

3.1 Functional specification

Specification of this model is designed to fit a large scale of operations in different scenarios. The input data is the power set point (Psp: positive in discharge mode and negative in charge mode) and output data are real battery power (Pb), state of charge (SOC), state of health (SOH), Joule losses, available discharge power and available charge power. (Figure 2)

As a physical battery, the following constraints must be satisfied:

- Charge power should not cause overvoltage ($V \leq Vmax$),
- Charging current does not exceed a limit value ($I \leq Ilim$).

In case of a discharge or charge power greater than the available value, the model will only provide its available power. Moreover, to preserve battery life-time, the model will decide to disconnect battery from electrical load when the state of charge is too low ($SOC = SOC_{min}$).

3.2 Electrical equivalent model

Various models are available in the literature [15] [17]to reach fine and fast simulation. In our framework, a simple model is preferred to describe charging and discharging process. This is the reason why we have chosen Shepherd’s hypothesis [12] as the basis content of this model. These hypotheses are based on a simple equivalent circuit: a voltage source is connected with a variable resistor. (Figure 3)

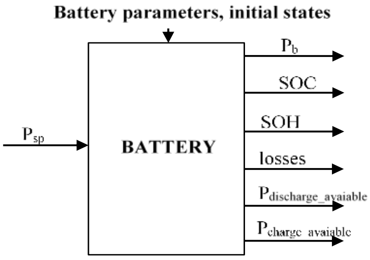

Figure 2. Battery model specification.

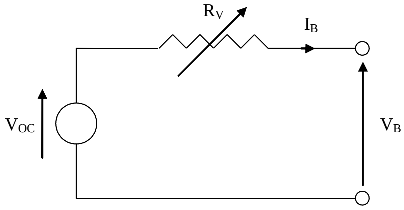

Figure 3. Electrical equivalent circuit.

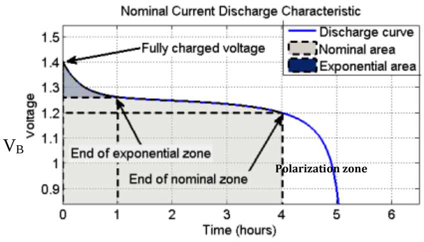

Figure 4. Typical Discharge Curve Characteristics.

This model must take into account the variation of battery voltage depending on battery state of charge. Indeed, the curve consists of three operating zones: exponential zone, nominal zone and polarization zone. (Figure 4)

By synthesizing the three discharge phenomena and Shepherd‘s hypothesis, we can re-establish power discharging and charging equations [13].

For the discharge mode ($I_B \geq 0$), the battery power equation across the battery can be defined as below:

$$P_B = V_0 I_B - R_I I_B^2 - K \frac{Q_{max}}{Q} I_B^2 + A\, I_B e^{B(Q-Q_{max})} \tag{4}$$

In charge mode ($I_B \leq 0$), the polarization resistor is modified to approach the operation of the battery. So the power equation is rewritten:

$$P_B = V_0 I_B - R_I I_B^2 - K \frac{Q_{max}}{Q_{max}-Q} I_B^2 + A\, I_B e^{B(Q-Q_{max})} \tag{5}$$

These equations allow determining the state of charge (SOC), the available powers (charge and discharge) and Joule losses.

State of charge:

$$SOC = \frac{Q}{Q_{nom}} \times 100\% \tag{6}$$

Joule losses in discharge mode:

$$Joule\ losses = R_I I_B^2 + K \frac{Q_{\max}}{Q} I_B^2 \tag{7}$$

Joule losses in charge mode:

$$Joule\ losses = R_I I_B^2 + K \frac{Q_{\max}}{Q_{\max}-Q} I_B^2 \tag{8}$$

Available discharge power:

$$P_{\text{discharge\_avaiable}} = \frac{[V_0 + A\, I_B e^{B(Q-Q_{\max}))}]^2}{4(R_I + K \frac{Q_{\max}}{Q})} \tag{9}$$

Available charge power at constant current stage:

$$P_{\text{charge\_avaiable}} = V_0 I_{\lim} - R_I I_{\lim}^2 - K \frac{Q_{\max}}{Q_{\max} - Q} I_{\lim}^2 + A\, I_{\lim} e^{B(Q - Q_{\max})} \quad (10)$$

Available charge power at constant voltage stage:

$$P_{\text{charge\_avaiable}} = -\frac{V_{\max}^2 - V_{\max} V_0 - V_{\max} A e^{B(Q - Q_{\max})}}{R_I + K \dfrac{Q_{\max}}{Q_{\max} - Q}} \quad (11)$$

Besides, the state of health (SOH) is estimated by "additive law" [17]:

$$SOH = \left[1 - \frac{\int |I_B| dt}{N_C \times Q_{\max}} \right] \times 100\% \quad (12)$$

The model can accurately simulate the behavior of an electric battery by using identified parameters from typical battery characteristics.

In our framework, we have to keep a compromise between accuracy and ease of use. In particular, model parameters can be considered constant in charge mode and discharge mode, thus facilitating the implementation of the model. Our model integrates the parameters for four famous kind of battery (Lead-acid, Ni-Cd, Ni-Mh, Li-ion).

3.3 Validation

3.3.1 Simulation in different modes

To survey available power in operation, the simulation test on Figure 5 illustrates set point powers for low and high demand for a battery with the following parameters: Ni-Cd, 4200mAh and initial SOC = 50%.

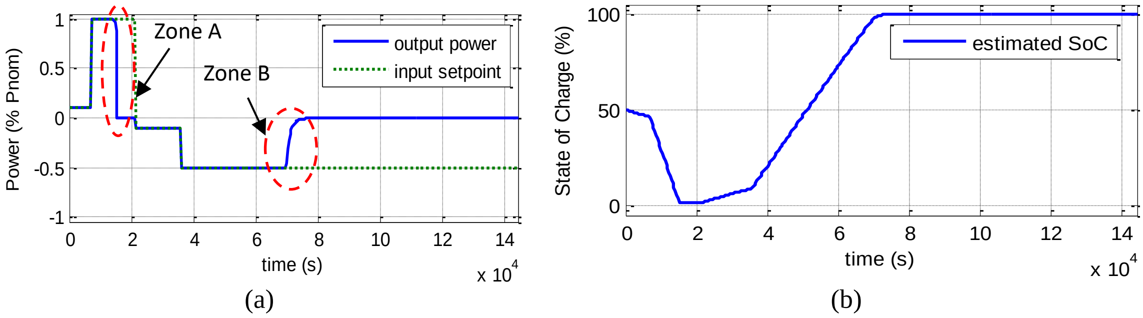

Figure 5. Power and state of charge in different modes.

Figure 5.a shows that the battery can provides a power that is lower than set point value (see zone A and zone B). Therefore, this demonstrates that our model allows calculating real battery power at the end of discharging or charging processes, this is important to decide the optimal control in building energy management.

3.3.2 Measurement vs Model

3.3.2.1 Simulation in different modes

This model is validated by a test on a Laptop DELL Latitude E6400 including a Li-ion battery (rated voltage: 11.1 V, rated capacity: 6100 mAh, cycle durability: 1200, initial state of charges 100%). Measurements are obtained by BatteryMon software (v2.1, www.passmark.com).

In Figure 6, the simulation is well reproducing the measured power set point and the measured state of charge. Because of using average parameters for Li-ion battery, the model cannot reproduce exactly the battery voltage which is sensible with different parameter values. This has an influence for calculating the state of charge which is sometimes a little bit higher or lower than measurement data. This is also the case for the output power which cannot reproduce exact values at the end of discharge mode or charge mode as shown on Figure 6.a.

For health protection, the battery should not be used until the end of its charge like it was done in this test case. Thus the peak estimated voltage at the end of battery charge (see Figure 6.b) would not exist in almost operation modes. Thus, if we exclude this peak value, Figure 6.b shows that the difference between simulations and measurements is lower than 10% which is the level of accuracy that we can accept.

3.3.2.2 Validation in terms of charge mode:

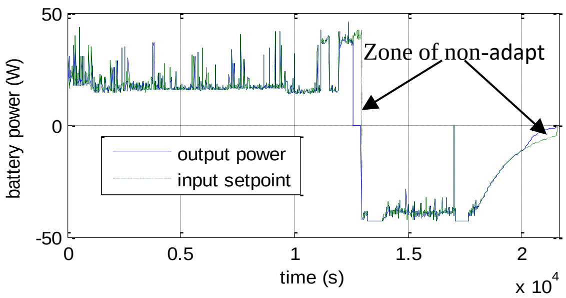

6(a)

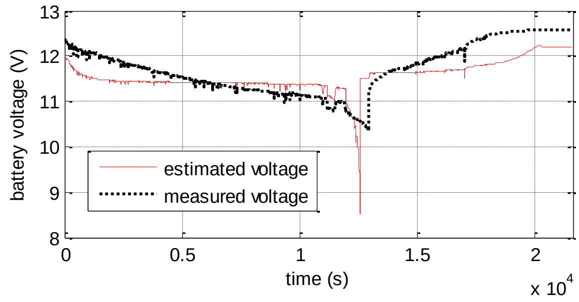

6(b)

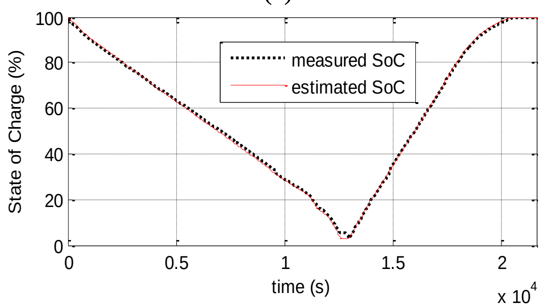

6(c)

Figure 6. Simulations vs measures for power, voltage and SOC.

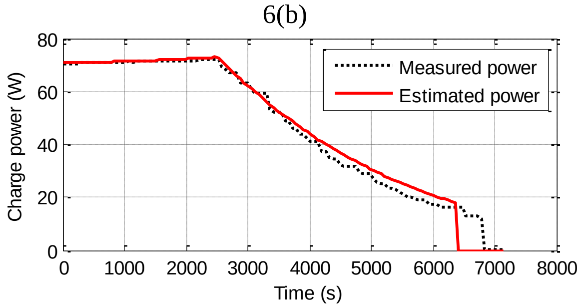

Figure 7. Model validation for power in charge mode.

Actually, the power set-point in charge mode of a laptop is not clearly defined. In fact, in almost cases, we usually estimate charge power of battery between the maximum power value of adapter and power consumption of the PC, while the real value depends completely on its properties (type of battery and technical parameters).

In order to validate battery model function in this condition, we made a test of charge mode (without using the PC) of a Li-ion battery from a computer: DELL PRECISION module KY265 11.1 V, battery capacity: 85 Wh, design charge power: 130.65 W (19.5 V × 6.7 A), the initial state of charge $SOC_0 = SOC_{min} = 5\%$, maximum charge current $I_{lim} = -0.7Q_{rat}$ and maximum voltage $V_{max} = 1.13V_{rat}$.

In Figure 7, the estimated power curve during charging is close to the battery characteristic curve. In constant current stage, the model calculation could well reproduce the measured power. But, in constant voltage stage, battery model start to make errors in calculation and they will be accumulated and lead to a different at end of charge process with an order of 7%. In our framework, these errors of charge power and charge state are acceptable for the purpose of prediction.

4. IMPLEMENTATION IN "PREDIS SMART BUILDING"

The PREDIS "smart building" (PREDIS SB) is situated in Grenoble Electrical Engineering Laboratory (France). It is a building used for researches on (building + grid) smart system. Battery modeling and control is one of research activities of this project.

To realize application of battery control strategy, a part of this platform is used as a computer room with laptops and controllable switches. We simulate a photovoltaic generation supply for the 15 laptops with a curve of generated power for 1 day illustrated on Figure 8. A command server sends wireless ON/OFF signal to each switch to decide charging/discharging mode of each laptop. The goal is to reach, or to be closer as possible from the photovoltaic autonomy [19]. Therefore, our objective is to define an autonomous and optimal control strategy by using battery model from a proposed scenario and initial battery states.

Technical details:

- Laptop DELL Precision, battery module KY265, type Li-ion, 11.1 V, 85Wh
- Photovoltaic panel: P_{max} = 1000W.

4.1 Simulation using models for prediction and real-time control

4.1.1 Forecast data

Our first application is realized by a simulation on a typical day in 2012 November. The total load (Figure 8) is summed from wattmeter measurements of each laptop at 100% state of charge in order to retrieve pure user load consumption (without battery charge consumption). Besides, the photovoltaic production is taken from measured data (Figure 9) and the electrical price is given by EPEX www.epexspot.com (Figure 10). State of charge for each battery is initialized to 100% by a full charging process, but the optimal control tries to reach the target of 50% SOC at the end of each day in order to have the possibility to charge or to discharge batteries.

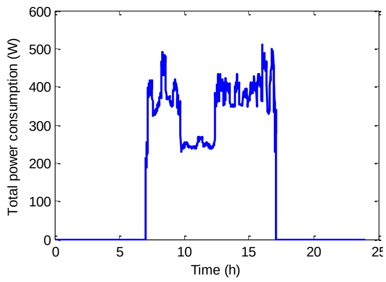

Figure 8. Total load consumption by laptop device.

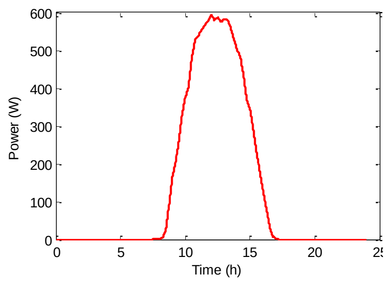

Figure 9. Photovoltaic power.

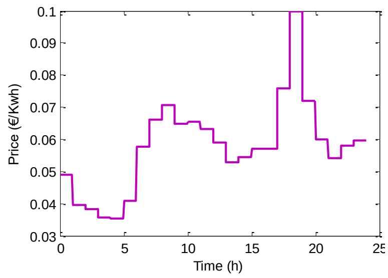

Figure 10. Electrical price.

4.1.2 Control strategy

To reach an optimal management, the control strategy must be deduced by following two steps: predictive and feedback control. The predictive control calculates energy balance from data prevision and allows preparing necessary energy in battery for whole day operations. In this case, the battery model is used to define charge time and to decide when each laptop should be charged from electrical price evolution. Further, the feedback control decides what laptop can be charged or discharged in each check-point time (each 6 minutes). For this goal, model is also used to calculate or predict battery states at next time.

4.1.3 Simulation results

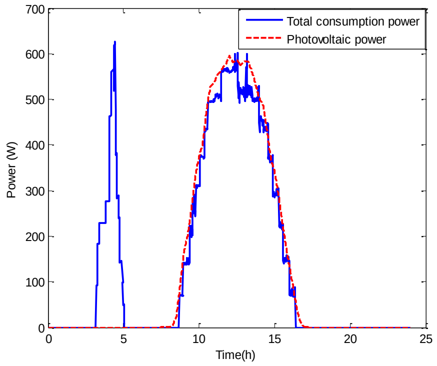

Figure 11. Total power consumption at electrical outlet and photovoltaic power.

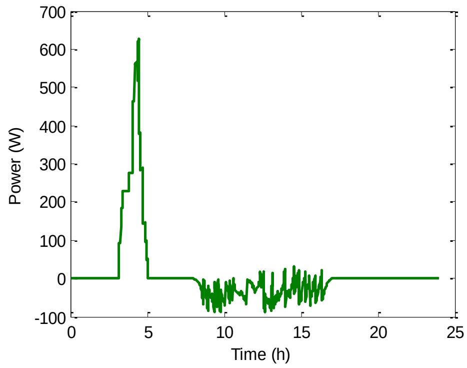

Figure 12. Electrical grid power.

Figure 11 shows total power consumption which is balanced with the photovoltaic production. By using batteries and an optimal control, the power consumption profile can benefit as much as possible from the generated power of the photovoltaic panel maximizing by this way the photovoltaic autonomy. Because the energy consumption in this case is more than the generated energy, this system need still to buy energy from electrical grid which is stored on laptop battery.

From Figure 12, the necessary power is bought at the cheapest moment (3:00am to 5:00am, from electricity variable prices of Figure 10) to minimize costs. Sometime, we can sell generated power to grid but in reality, this power is used locally for other consumptions (HVAC, lighting…). To understand the gains of this application, the table below compares our strategy to the classical case (PC without electrical storage). The cost gain is about 10 times.

4.2 Application in real the system

The previous part was done for a simulated system in order to developed models and optimal control algorithm. In this section, we have applied the optimal control on the real system.

4.2.1 Control devices

In this section, we introduce control materials in our control protocol: command server, receiver and transmitter RF module, controlled outlet, Zigbee wattmeter and virtual sensor (Figure 13).

By integrating the control module and the management module data, our home abstraction layer (HAL) server allows retrieving measured data and control actuators in order to manage energy devices and especially energy storage system of laptops.

Besides, receiver and transmitter RF module communicates to command server on TCP / IP connection. This module converts RF frames to PLC signals (power line communication) which are transferred on the electrical grid, in order to turn on or off the controlled outlets.

Zigbee wattmeter and controlled outlet are inserted between the network electrical and laptop adapter (Figure 14)

- Zigbee wattmeter measures power consumption and sends it via Xbee gateway, which is connected to the server by USB interface port.
- The controlled outlet receives ON/OFF signals via electrical grid by PLC.

Measured battery status (SOC, SOH ...) is got from software BatteryViewInfo (Figure 15) (www.nirsoft.net).

This software allows exporting data in several types (*. Txt, *. html*. xml ...), which are very easy to operate through the TCP/IP network. Thus, this software is considered a "sensor virtual " because it produces quantities that are not directly measured such as current capacity (%).

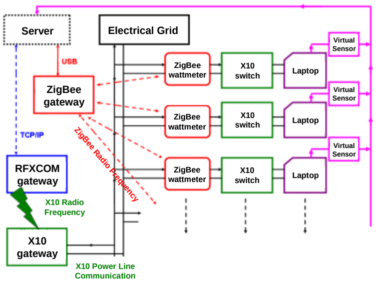

Figure 13. Communication network.

Figure 14. Electrical power meter and receiver (Zigbee radio frequency).

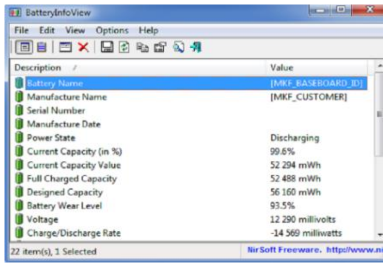

Figure 15. Battery monitoring tool

4.2.2 Real system results

The optimal controller has been installed into the command server and is able to call model simulation for prediction phase, as well as real-time monitoring and control using HAL server. Results obtained during a day are the followings.

In Figure 16, we can notice that batteries charging have been realized early on the morning and that power taken from electrical outlet follows photovoltaic production. In Figure 17, we can see batteries charging and discharging power, as well as computers load.

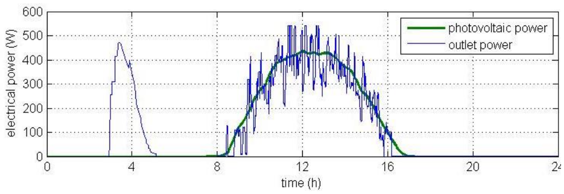

Figure 16. Photovoltaic production ant electrical outlets power

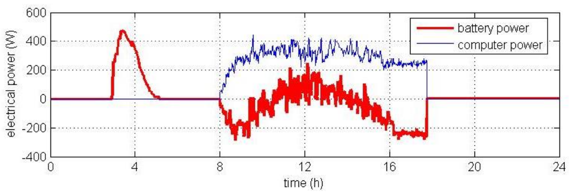

Figure 17. Batteries power (charge and discharge) and computers load.

Fig. 18, is detailing batteries state of charge (SOC). Before class starting, batteries are full of charge. At 8 o'clock, some PC start running discharging their battery. After some minutes, photovoltaic production is enough to supply energy to some PC. From 11 am to 2 pm, there is an amount of energy which supply computer load as well as charging of batteries. From 2 pm to 6 pm, batteries are discharging due to insufficient production. At the end of the day, batteries SOC are very low which is due to an intensive use of computer during.

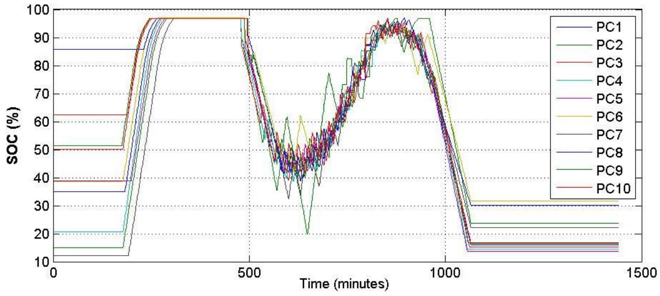

Figure 18. Laptops battery state of charge on real system

5. RESULTS AND DISCUSSION

Based on ideas and results of this research, under the cooperation between USTH, HIT, G2Elab and IES-VAST, we are deploying the "Micro Smart Grid Development and Application for Building Energy Management" project in order to approach two new research directions: building energy management and micro smart grid [20]. In fact, our research focuses on the Micro Smart Grid development at the local level (building) that is estimated to last for a period of 3 years (2015 – 2018). The 5th floor and 6th floor (with four labs and a classroom) of USTH building, where we can carry out experimental simulation model in a real case, have been chose to be the research platform. Besides, the power supply system will be from a photovoltaic energy source, an electrical storage (battery energy storage station - Lithium batteries blocks of LiFePO4), and EVN power grid (low voltage). Indeed, the photovoltaic generation system at power scale of 15 kWp including an inverter and solar panels will be installed on the rooftop of USTH building. This PV system extracts maximum power from the PV arrays and injects maximum power into grid in various conditions. The load includes in this case single phase and triple phase namely lighting systems, heating ventilation and air-conditioning systems (HVAC systems), and elevator of USTH building. Moreover, we will utilize another bank called "load bank". It allows the simulation of resistive, inductive and capacitive loads and provides for the research in different conditions in the smart grid platform. Besides that, the monitoring system (energy meters, PLCs and SCADA) allows collecting data that can be analyzed providing information for the optimal operation. The energy controller reads all the data measured by the transducers for managing and running the equipment following the different selected modes. The energy manager controls the delivery of energy, the run of charges and discharges batteries.

6. NOMENCLATURE

Symbol	Signification
PPV	Photovoltaic power (W)
ηg	Instantaneous PV generator efficiency
N	Number of cell
Am	Surface of one cell
Gt	Solar irradiance
ηr	Reference maximal efficiency
ηpt	Power operation efficiency

ns	Number of students
Bt	Efficiency coefficient
Ta	Ambient temperature
Tr	Reference temperature
NOCT	Nominal operation cell temperature
$V_{OC} = V_0 + A\, e^{B(Q-Q_{max})}$	Open circuit voltage (V)
$R_V = R_I + K \frac{Q_{max}}{Q}$	Variable resistor (Ω)
V0	Constant voltage (V)
RI	Internal resistor (Ω)
K	Polarization voltage factor (V)
IB	Battery intensity (A)
Qmax	Maximum capacity (Ah)
Q0	Initial charge (Ah)
$Q = Q_0 - \eta_C \int_0^t I_B dt$	Instantaneous charge (Ah) 16
ηC	Faraday efficiency
A	Voltage factor (V)
B	Charge factor (Ah-1)
NC	Cycle durability

Acknowledgements. The research was realized in Grenoble Electrical Engineering Laboratory, under the supervision of Prof. Benoit Delinchant and Prof. Frederic Wurtz.

REFERENCES

1. Medina, J. ; Muller, N. ; Roytelman, I. “Demand Response and Distribution Grid Operations: Opportunities and Challenges”, IEEE Transactions on Smart Grid, Volume: 1 , Issue: 2, pp 193 – 198, 2010Tewari P. K., Singh R. K., Batra V. S., and Balakrishnan M. - Membrane bioreactor (MBR) for wastewater treatment, Sep. Pur. Tech. 71 (4) (2010) 200-204.
2. Kupzog, F. ; Roesener, C., “A closer Look on Load Management”, Proceedings of The 5th IEEE International Conference on Industrial Informatics, Volume: 2, pp 1151 – 1156, 2007.
3. Hadjsaid, N. ; Canard, J.-F. ; Dumas, F. “Dispersed generation impact on distribution networks”, IEEE Computer Applications in Power, Volume: 12 , Issue: 2, pp 22 – 28, 1999.
4. Siano, P. ; Cecati, C. ; Hao Yu ; Kolbusz, J. “Real Time Operation of Smart Grids via FCN Networks and Optimal Power Flow”, IEEE Transactions on Industrial Informatics, Volume: 8 , Issue: 4 pp 944 – 952, 2012.
5. Conejo, A.J. ; Morales, J.M. ; Baringo, L. “Real-Time Demand Response Model”, IEEE Transactions on Smart Grid, Volume: 1 , Issue: 3, pp 236 – 242, 2010.
6. De Angelis, F. ; Boaro, M. ; Fuselli, D. ; Squartini, S. ; Piazza, F. ; Qinglai Wei “Optimal Home Energy Management Under Dynamic Electrical and Thermal Constraints”, IEEE Transactions on Industrial Informatics, Volume: 9 , Issue: 3, pp 1518 – 1527, 2013.

7. Sortomme, E. ; El-Sharkawi, M.A. “Optimal Charging Strategies for Unidirectional Vehicle-to-Grid”, IEEE Transactions on Smart Grid, Volume: 2 , Issue: 1, pp 131 – 138, 2011.
8. Sortomme, E. ; El-Sharkawi, M.A. “Optimal Scheduling of Vehicle-to-Grid Energy and Ancillary Services”, IEEE Transactions on Smart Grid, Volume: 3 , Issue: 1, pp 351 – 359, 2012.
9. Markvard, T., 2000. Solar Electricity, second ed. Willey, USA.
10. S. Diafa, D. Diaf, M. Belhamel, M. Haddadi, A. Louche. June 2007. A methodology for optimal sizing of autonomous hybrid PV/wind system, Energy Policy 35 (2007) 5708-5718.
11. Celik, A.N. Dec 2002. Optimization and techno-economic analysis of autonomous photovoltaic–wind hybrid energy systems in comparison to single photovoltaic and wind systems, ScienceDirect, volume 43, issue 18, pages 2453-2468.
12. Shepherd, C.M. May 2 1963. Theoretical design of primary and secondary cells, part III - battery discharge equation, internal report, U. S. naval research laboratory.
13. Tremblay, O., Dessaint, L.A., Dekkiche, A.I. Sept 9-12 2007. A Generic Battery Model for the Dynamic Simulation of Hybrid Electric Vehicles, IEEE VPPC 2007, pages 284 – 289.
14. Tremblay, O., Dessaint, L.A May 13-16 2009. Experimental Validation of a Battery Dynamic Model for EV, World Electric Vehicle Journal, volume 3, SSN 2032-6653.
15. Guasch, D., Silvestre, S. May 2003. Dynamic Battery Model for Photovoltaic Applications, Progress in Photovoltaic: Research and Applications, Volume 11, Issue 3, pages 193–206.
16. Valøen, L.O., Shoesmith, M.I., Nov 2007. The effect of PHEV and HEV duty cycles on battery and Battery Park performance, PHEV 2007 Conference, Winnipeg, Manitoba Canada.
17. Long L. Aug 23 2011. A Practical Circuit based Model for State of Health Estimation of Li-ion Battery Cells in Electric Vehicles, Master of Science thesis, TU Delft, Netherlands.
18. Picciano N. 2007. Battery Aging and Characterization of Nickel Metal Hydride and Lead Acid, The Ohio State University, USA.
19. Kazema H. A., Khatiba T., Sopianb K., June 2013. Sizing of a standalone photovoltaic/battery system at minimum cost for remote housing electrification in Sohar, Oman, Energy and Buildings, Vol. 61, pp 108–115.
20. Delinchant B., Nguyen X.T., Nguyen D.Q., Dang H.A., Wurtz F., June 2015. Micro Smart Grid Development and Application for Building Energy Management. 2015 USTH Research project description.